Multi-output Auxiliary Power Supply with Lossless Snubber

Geeng-Kwei Chang Shu-Yuan Fan
Department of Electrical Engineering
Wufeng University
Ming-Hsiung, Chia-Yi, Taiwan, R.O.C
e-mail: gkchang@wfu.edu.tw

Sheng-Yu Tseng
Green Power Evolution Applied Research Lab (G-PEARL)
Department of Electrical Engineering
Chang Gung University
Kwei-Shan, Tao-Yuan, Taiwan, R.O.C
e-mail: sytseng@mail.cgu.edu.tw

Abstract: - A multi-output auxiliary power supply realized by a flyback converter is presented for providing the essential low power supplies for control circuits and driving circuits in power processing systems. In the proposed circuit topology, lossless snubbers are introduced into the flyback converter to recover energy trapped in leakage inductor of transformer, and as a result, smoothes out voltage surge across drain-source of the switch, and alleviates oscillation caused by parasitic capacitance of the switch and leakage inductance of the transformer, hence reduces switching losses and improves conversion efficiency. Based on these concepts, an auxiliary power supply with five sets of output voltage has been designed and implemented to verify the feasibility of the proposed multi-output auxiliary power supply. Experimental results show that the conversion efficiency has been increased about 5% and reached 82.5% under full load as compared with flyback converter with hard-switching.

Key-Words: - flyback converter; lossless snubber; auxiliary power supply.

1 Introduction

Power processing systems play a major role in today's electric utilities, for instance, in solar power generation systems, in power unit of electric vehicles, in battery chargers, in space satellites, in uninterruptible power supplies (UPS), in active power filters, etc. In the power processing systems, the auxiliary power supply is needed to provide different voltages for the control circuits and driving circuits. The needed voltages are ranged from 3.3V to 24V. Two different design concepts are available, one is low-frequency ac transformer, and the other is high-frequency switch-mode power supply (SMPS) [1, 2]. Although the ac transformer can provide stable and independent power source, it is bulky and uneasy to install on circuit board. On the other hand, SMPS, been compact in weight and size and more efficiency, is finding increased attention in industry and academia as one of the preferred choices for low-power application. SMPS has successfully made its way into the industry and is now a mature and proven technology. Many kinds of converters can be used to realize the SMPS, such as half-bridge converter, full-bridge converter, push-pull converter, flyback converter or forward converter [3], and so on.

Among various selecting criteria for an appropriate converter, galvanic insulation is an decisive one when insulation from power line is recommended. Since the auxiliary power supply takes input voltage from power line and has to provide several regulated and isolated dc output voltages with different levels, the galvanic insulation becomes the most important

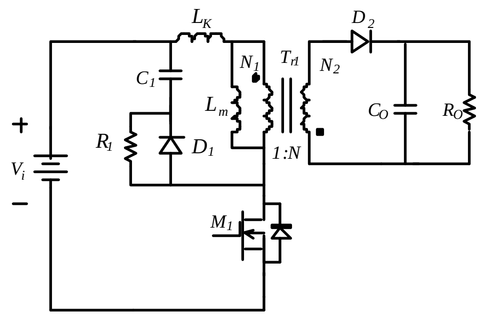

Fig. 1. Schematic diagram of flyback converter with conventional RCD snubber.

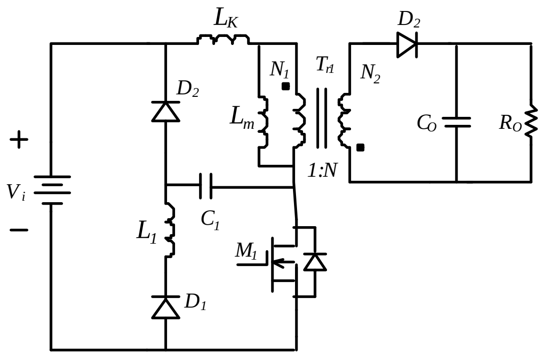

Fig. 2. Schematic diagram of flyback converter with lossless LCD snubber.

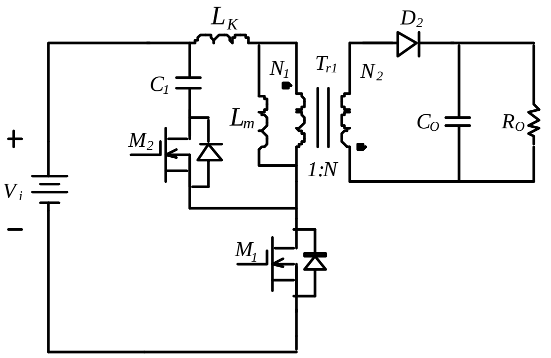

Fig. 3. Schematic diagram of flyback converter with conventional active clamp circuit.

factor to be taken into consideration. Hence, flyback type or forward type converter with multiple outputs coupled magnetically through transformer are more suitable for auxiliary power applications [4].

In reality, no matter how one arranges the winding structure inside the transformer, it brings about leakage inductance. As a result, a flyback converter generally suffers from low efficiency and voltage surge across power transistor switches. To reduce voltage surge, an RC clamp circuit is usually inserted to absorb the energy stored in the leakage inductance and suppress the spike. This absorbed energy is dissipated in the snubber resistor during transistor turn-on. To increase the efficiency, a non-dissipative LC clamp circuit was proposed. In the circuit, the absorbed energy is returned through the snubber inductor to the power source [5-7]. Both of the aforementioned circuit do not consider the diode reverse recovery effects which may cause the oscillation in voltage surge during switching, RCD as well as RC-RCD clamp circuits are proposed [8-11]. A typical RCD snubber is shown in Fig. 1. With the RCD snubber, spike voltage across switch is reduced, but additional power loss is generated. In Fig. 2, a lossless LCD snubber is used to replace RCD snubber to increase the conversion efficiency. Since RCD and LCD snubber can only improve voltage surge across switch to reduce switching loss, it does not increase

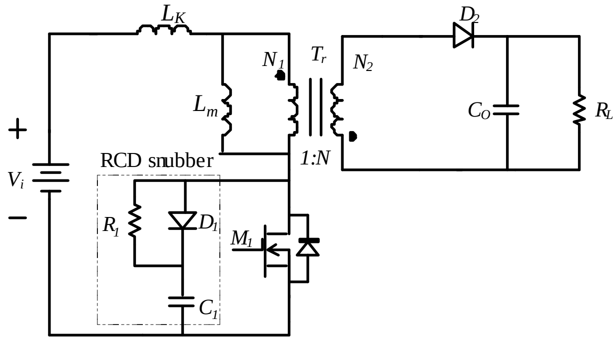

Fig. 4. Schematic diagram of flyback converter with conventional RCD snubber in parallel with the

conversion efficiency. Therefore, as shown in Fig. 3, an active clamp circuit composed of an active switch is introduced into the flyback converter. Besides of resetting the transformer and suppressing the surge, the circuit can store and release the surge energy at adequate timing through the active switch to raise efficiency and achieve soft-switching [12-14]. Although the active clamp circuits can increase conversion efficiency of converter, it needs extra driving circuit and active switch, resulting in a higher cost. Hence, a lossless snubber shown in Fig. 4 is proposed to recover energy trapped in leakage inductor and reduce switching losses. As shown in Fig. 4, the proposed lossless snubber is composed of passive components only and can achieve a lower cost.

A variant of the RCD type snubber is adopted for the multi-output flyback converter. The RCD snubber in Fig. 1 can be placed in parallel with the switch, as shown in Fig. 4. In order to recover the energy trapped in leakage inductor of transformer, the resistor R_1 in the RCD snubber can be replaced by a transformer coupled to the output, resulting in the circuit in Fig. 5. It can be seen that the proposed snubber can recover the energy trapped in leakage inductor to output load and thus increases the overall

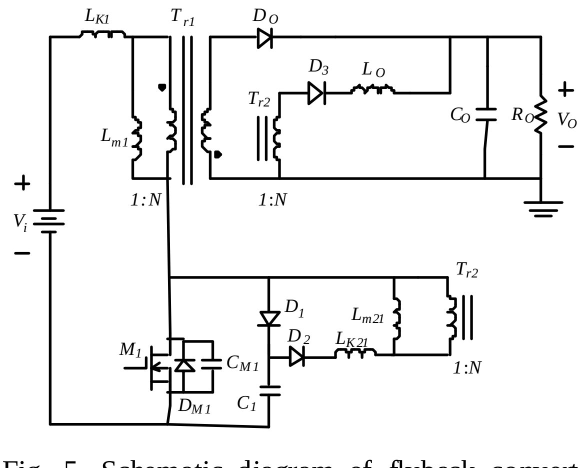

Fig. 5. Schematic diagram of flyback converter with the proposed lossless snubber.

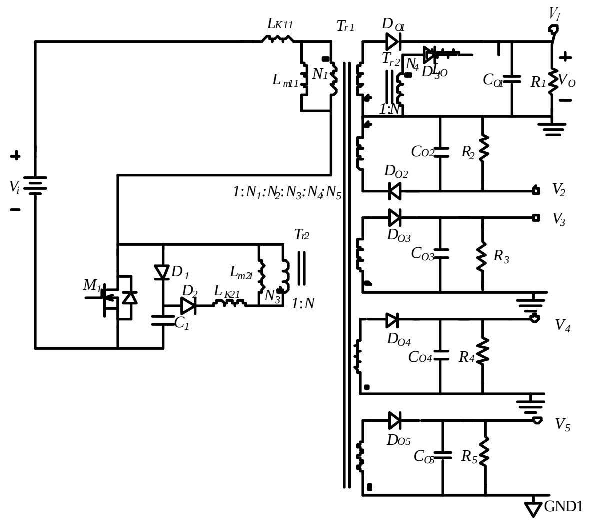

Fig. 6. Schematic diagram of the proposed auxiliary power supply with five sets of output voltages.

efficiency. Fig. 6 shows the complete circuitry with five sets of output.

2 Operational Principles of the Proposed Auxiliary Power Supply

In order to simplify the analysis of the proposed snubber, the one output converter as shown in Fig. 5 is considered in the analysis. Operation of this circuit can be divided into seven operation modes, and suppression of transistor surge voltage is different in each mode. In Fig. 7, (a)~(g), the operational principles corresponding to each mode are illustrated. From the key waveforms shown in Fig. 8, the detail operation of this converter can be clarified.

Mode 1 [Fig. 7(a); $t_0 \le t < t_1$]

Before time t_0, the switch M_1 is OFF, diode D_1 is on, and the energy stored in the primary windings of transformer T_{r1} is transferring to the secondary windings and the load through diode D_o. At $t = t_0$, switch M_1 is turned on. At this instance, voltage across the magnetizing inductor L_{m11} is

$$V_{N1} = -\frac{V_O}{N} = L_{m11}\frac{di_{Lm11}}{dt} \quad (1)$$

while the voltage across the leakage inductor L_{K11} is

$$V_{LK11} = V_i + \frac{V_O}{N} = L_{K11}\frac{di_{LK11}}{dt} \quad (2)$$

Since the leakage inductance is smaller than the magnetizing inductance, one can find that, from the above two equations, the current I_{LK11} increases rapidly while the current I_{Lm11} decreases linearly. However, as long as I_{Lm11} be greater than I_{LK11}, diode D_o keeps forward biased, which makes transformer T_{r1} continue transferring its energy to the load.

Additionally, before t_0, voltage across capacitor C_1 reaches the level $(V_i + V_o / N)$, higher than V_o / N, which, when switch M_1 is ON, been applied across the primary winding of transformer T_{r2}, will make diodes D_2 and D_3 forward biased. Thus, energy stored in capacitor C_1 can be transferred to the output through diode D_3. Meanwhile, the circuit including diodes D_2 and D_3 is equivalent to an LC circuit (suppose that V_o is constant), and current i_{D3} will resonant from zero to a positive value, then back to zero while cut off diode D_3.

Mode 2 [Fig. 7(b); $t_1 \le t < t_2$]

At t_1, I_{LK11} equals I_{Lm11} and I_{N1} equals zero, which makes the diode D_o reversely biased. The input side circuit behavior is dominated by

$$V_i = (L_{K11} + L_{m11})\frac{di_{LK11}}{dt} \quad (3)$$

That is, within this time interval, $I_{Lm11} = I_{LK11}$ increases linearly and transformer T_{r1} is storing energy. The capacitor C_1 keeps releasing its energy to the load through diode D_2 、 transformer T_{r2} and diode D_3. This mode ends when diode D_3 is OFF.

Mode 3 [Fig. 7(c); $t_2 \le t < t_3$]

This mode begins at t_2 when diode D_3 is OFF. In this mode, both transformers T_{r1} and T_{r2} are storing energy, T_{r1} from the source V_i and T_{r2} from the capacitor C_1. This mode ends when the energy stored in capacitor C_1 is completely released.

Mode 4 [Fig. 7(d); $t_3 \le t < t_4$]

At t_3 the energy stored in the capacitor C_1 is completely released. In this circumstances, the magnetizing energy stored in transformer T_{r2} is freewheeling through diodes D_1 and D_2. The transformer T_{r1} is still in its energy storage stage and the magnetizing current I_{Lm11} increases linearly.

Mode 5 [Fig. 7(e); $t_4 \le t < t_5$]

At $t = t_4$, switch M_1 is turned off. At this moment, the inductor current $I_{Lm11} = I_{LK11}$ is sustained in continuous through the parasitic capacitor C_{M1} as well as diode D_1 and capacitor C_1. Since the capacitance of C_1 is greater than the capacitance of C_{M1}, the charging process of C_1 will make the voltage across switch M_1 increase smoothly, from 0 to $(V_i + V_o / N)$ and beyond. Therefore, switch M_1 can

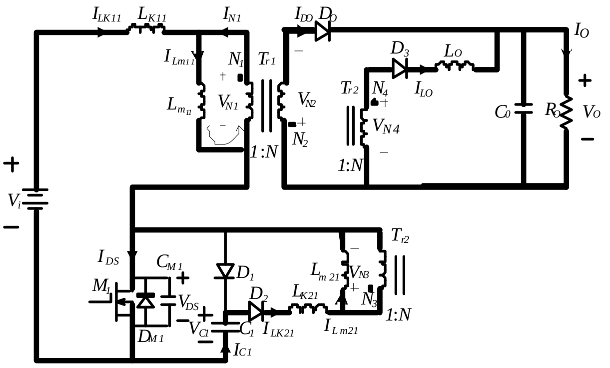

Fig. 7(a). Mode 1

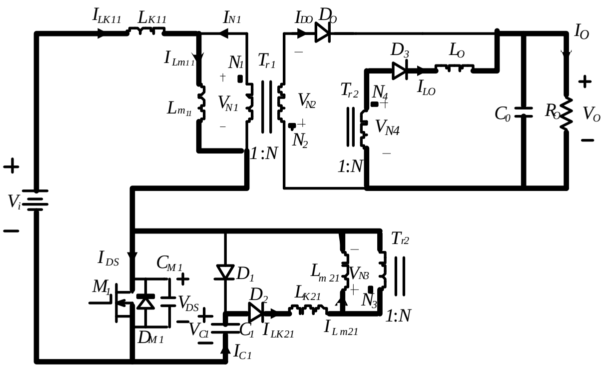

Fig. 7(b). Mode 2

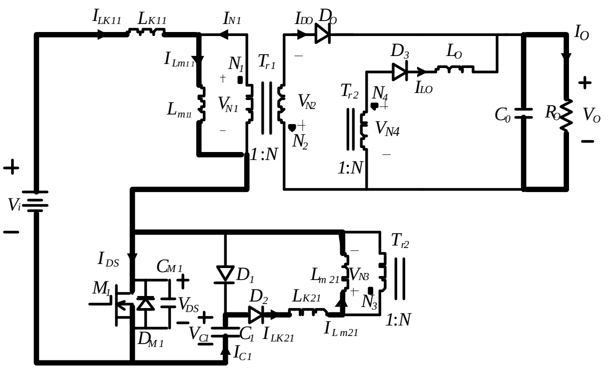

Fig. 7(c). Mode 3

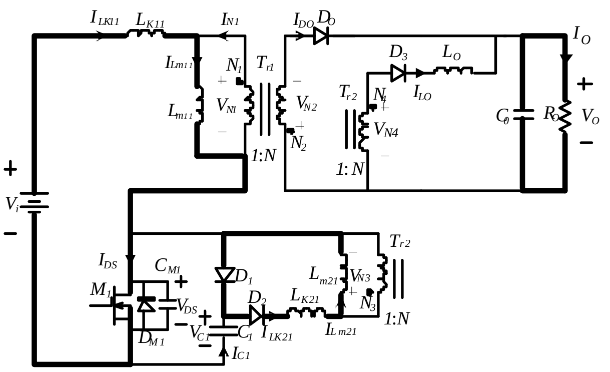

Fig. 7(d). Mode 4

Fig. 7. Operational principle of the proposed converter

be operated with zero-voltage transition (ZVT). Diodes D_1 and D_2 are still in freewheeling condition through inductors L_{m21}.

Mode 6 [Fig. 7(f); $t_5 \le t < t_6$]

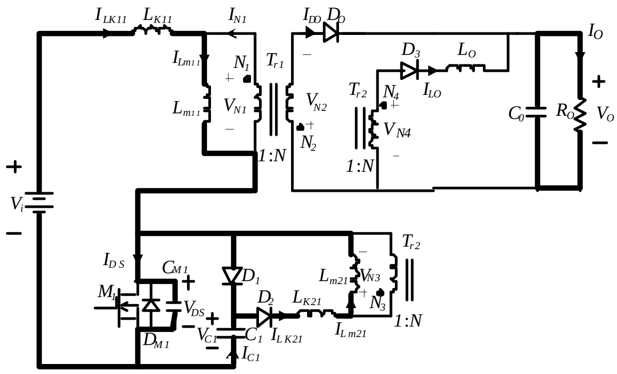

Fig. 7(e). Mode 5

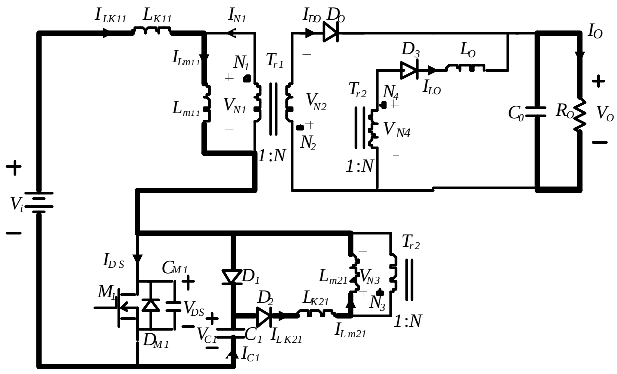

Fig. 7(f). Mode 6

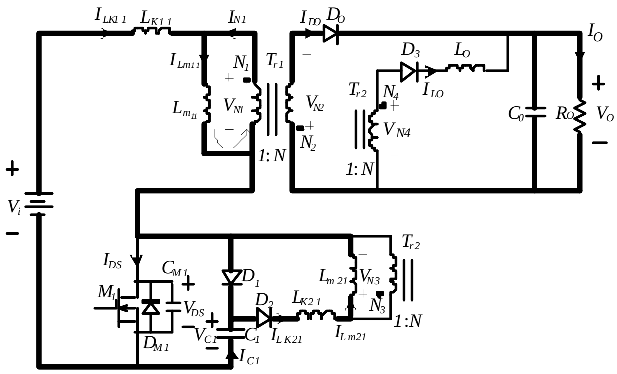

Fig. 7(g). Mode 7

Fig. 7. Operational principle of the proposed converter (continued)

At t_5, I_{DS} reaches zero, switch M_1 is completely OFF. $I_{Lm11} = I_{LK11}$ continues charging C_1.

Mode 7 [Fig. 7(g); $t_6 \le t < t_7$]

At t_6, voltage across capacitor C_1 reaches $(V_i + V_o / N)$, which makes diode D_o forward biased. Current i_{Do} will resonant to the value of I_o. The energy stored in the transformer T_{r1} will be released to the load through D_o, which makes current I_{Lm11} decreasing linearly. On the other hand, $I_{LK11} = I_{Lm11} - I_{N1} = I_{Lm11} - \dfrac{i_{Do}}{N}$ will resonant from the value of I_{Lm11} to zero while charging the

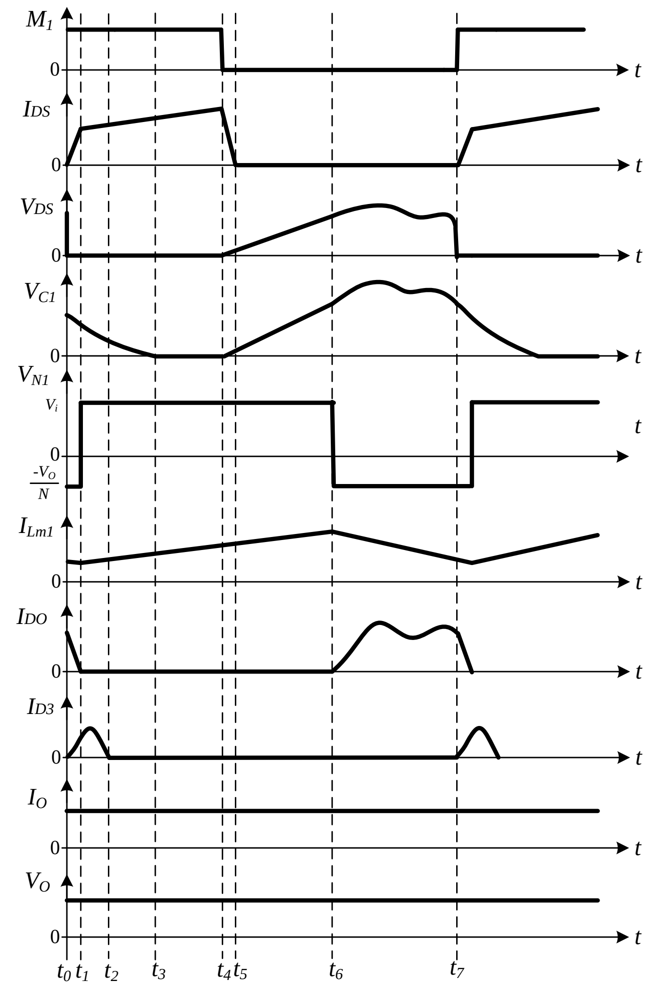

Fig. 8. Key waveforms of the proposed converter.

capacitor C_1 to a voltage value higher than $(V_i + V_o / N)$, which keeps the diode D_o in its forward biased condition. Meanwhile, L_{m21} keeps in freewheeling condition. When switch M_1 is turned on at the end of mode 7, a new switching cycle starts.

3 Design of the Proposed Auxiliary Power Supply

To design the proposed power supply systematically, determination of duty ratio D, transformers T_{r1} 、 T_{r2} and capacitor C_1 are detailed as follows [14].

3.1 Duty ratio D

As the converter is operating in continuous conduction mode (CCM) and, according to volt-second balance principle, the following equation can be obtained:

$$V_i DT_S + (\frac{-V_O}{N})(1 - D)T_S = 0 \tag{4}$$

where T_S is the switching period of M_1, N is the turns-ratio of transformer T_{r1}, while V_i and V_o are the input and output voltage respectively as shown in Fig. 7. From (4), it can be found that transfer ratio M can be expressed as

$$M = \frac{V_o}{V_i} = \frac{ND}{1-D} \tag{5}$$

According to (5), although the duty ratio D can be determined once the transfer ratio M and turns-ratio N are specified, it is important to consider the relationships between duty ratio and component stress. Referring to (5), a larger duty ratio D corresponds to smaller transformer turns-ratio N, which results in a lower current stress imposed on switch M_1, as well as lower voltage stress on freewheeling diode D_o. In order to accommodate load variations, line voltage, component value, a suitable operating range of duty ratio is between 0.35 and 0.4.

3.2 Transformers T_{r1}

Once the duty ratio is selected, the turns-ratio of transformer T_{r1} can be determined from (5), which is

$$N = \frac{(1-D)V_o}{DV_i} \tag{6}$$

By applying the Faraday's law, the number N_1 of turns at the primary winding can be determined as

$$N_1 = \frac{DV_i T_s}{A_c \Delta B} \tag{7}$$

where A_c is the effective cross-section area of the transformer core and ΔB is the working flux density. According to (6) and (7), the number of turns of secondary winding N_2 can be determined.

For the flyback converter, magnetizing inductor L_{m11} of the transformer is determined by taking into account the current down slope, which corresponds to the off-time of switch M_1, and the inductance must be large enough to maintain continuous conduction mode (CCM) operation. The inductance of L_{m11} must satisfy the following inequality:

$$L_{m11} \geq \frac{V_o(1-D)T_s}{N^2 \Delta I_{Do(\max)}} \tag{8}$$

where $\Delta I_{Do(\max)}$ is the maximum ripple of the secondary winding current of transformer T_{r1} that goes through diode D_o, and it is equal to $\Delta I_{Lm11(\max)}/N$. When the maximum current ripple is specified, the minimum magnetizing inductance can be determined.

3.3 Capacitor C_1

In the propose lossless snubber, capacitor C_1 is used to store the energy from the leakage inductance and to eliminate the switch turn-off loss. The energy stored in C_1 can be determined as

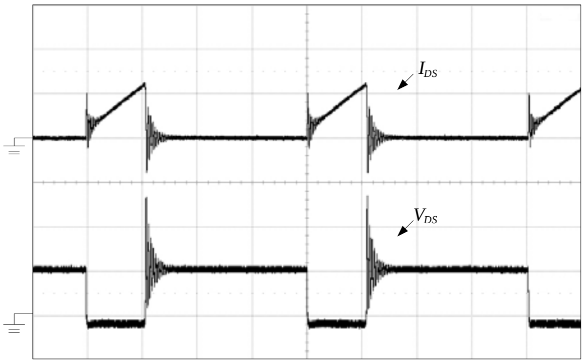

(V_{DS}: 50 V/div, I_{DS}: 1 A/div, 5 μs/div)
(a)

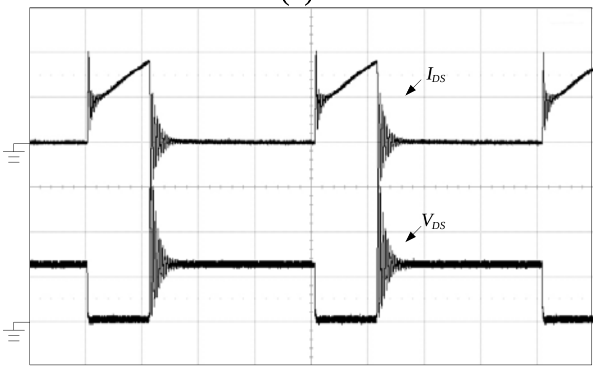

(V_{DS}: 50 V/div, I_{DS}: 1 A/div, 5 μs/div)
(b)

Fig. 9. Measured voltage V_{DS} and current I_{DS} waveforms of switch M_1 of the proposed auxiliary power supply under hard-switching (a) under 50%, and (b) under 100% of full load.

$$W_{C1} = \frac{1}{2} C_1 (V_i + \frac{V_o}{N})^2 \tag{9}$$

To completely eliminate the switch turn-off loss, the energy stored in capacitor C_1 must at least equal to the turn-off transition loss W_{Soff} , which is expressed as

$$W_{Soff} = \frac{t_{Soff}}{2} (V_i + \frac{V_o}{N}) I_{DP} \tag{10}$$

where t_{Soff} is the turn-off transition time of switch M_1 and I_{DP} is the current passing the switch. Therefore, from (9) and (10), capacitor C_1 can be determined as

$$C_1 \geq \frac{t_{Soff} I_{DP} (V_i + \frac{V_o}{N})}{(V_i + \frac{V_o}{N})^2} \tag{11}$$

4 Measured Results

To verify the performance of the proposed auxiliary power supply, a prototype with the following specifications is implemented.

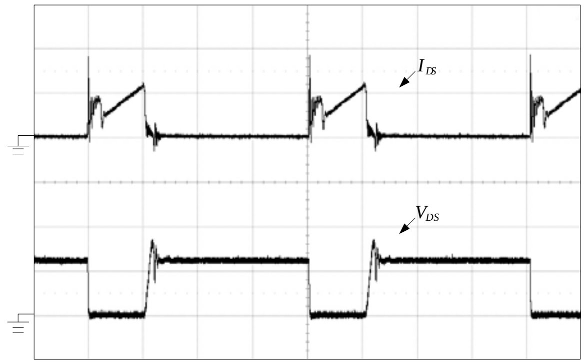

(V_{DS}: 50 V/div, I_{DS}: 10 A/div, 5 μs/div)
(a)

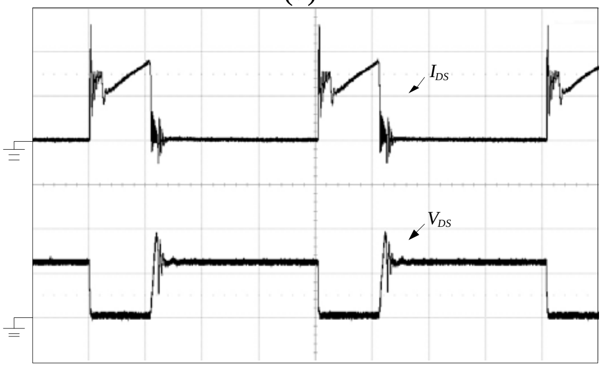

(V_{DS}: 50 V/div, I_{DS}: 10 A/div, 5 μs/div)
(b)

Fig. 10. Measured voltage V_{DS} and current I_{DS} waveforms of switch M_1 of the proposed auxiliary power supply with lossless snubber (a) under 50%, and (b) under 100% of full load.

- input voltage V_i : 48 V_{dc}
- output voltage V_o : +15 V_{dc} , -15 V_{dc} , +5 V_{dc} , +18 V_{dc} and an isolated +15 V_{dc}
- switching frequency f_s : 50 kHz
- maximum output current I_o : 1 A, 0.2 A, 0.6 A, 0.17 A and 0.2 A
- maximum output power P_o : 30 W

According to the specifications, components of the proposed auxiliary power supply are determined as follows:

- turns-ratio of transformer T_{r1} : 1:3:3:1.5:3.5:3
- magnetizing inductance L_{m11} : 147 μH
- leakage inductance L_{K11} : 0.9 μH
- transformer core: EI-33
- capacitor C_1 : 39 nF
- switch M_1 : IRFPS59N60C

Measured waveforms of V_{DS} and I_{DS} of switch M_1 of the proposed auxiliary power supply under hard-switching are shown in Fig. 9. Fig. 9(a) shows those waveforms under 50% of full load while Fig. 9(b) shows those waveforms under full load. Wave-

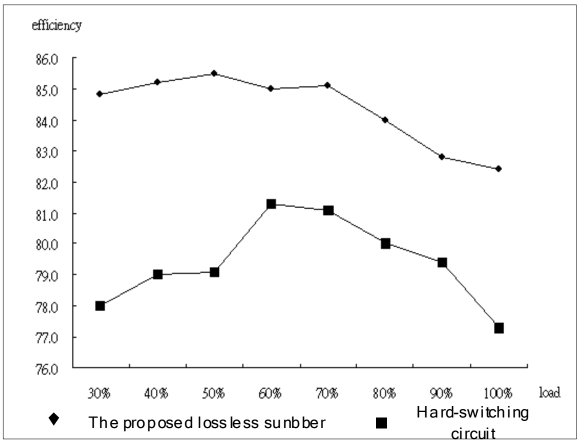

Fig. 11. Comparison of efficiency between the proposed auxiliary power supply under hard-switching and with the proposed lossless snubber from light load to heavy load.

forms shown in Fig. 10 are the same waveforms except that the proposed lossless snubber is applied. From Fig. 9 and Fig. 10, it can be seen that the power supply with the proposed lossless snubber can reduce surge voltage across transistor switch at turn-on (ZVS) and decrease slew rate of voltage across the switch at turn-off (ZVT). Comparison of conversion efficiency between the power supply under hard-switching and with the proposed lossless snubber from light load to heavy load is shown in Fig. 11. From Fig. 11, it is clear that the efficiency of the proposed one is higher than that under hard-switching, and its efficiency reaches 82.5% under full load condition.

Fig. 12 shows measured waveforms of output voltage V_o and current I_o of the proposed power supply under a step-load change between 20% and 100% of full load. From Fig. 12 it can be observed that voltage regulation of output voltage V_o of 15V is limited within ±1%.

5 Conclusion

In this paper, some traditional snubber circuits have been briefly reviewed, and an lossless snubber is introduced to a flyback type multi-output auxiliary power supply to reduce the surge voltage across the power switch as well as recover the energy trapped in leakage inductor to output load to increase the overall efficiency. Operational principle, steady-state analysis and design procedures are detailed in the article. Experimental results revealed that the proposed lossless snubber can reduce surge voltage across transistor switch at turn-on and decrease slew rate of voltage across the switch at turn-off. Furthermore, it can achieve high efficiency over a wide load variation range and exhibit good voltage regulation characteristic.

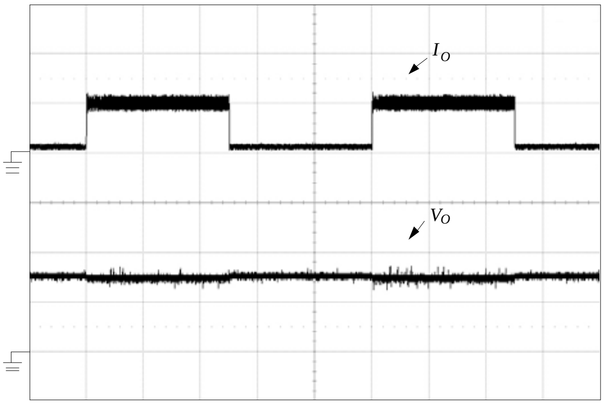

(V_O: 10V/div, I_O: 1 A/div, 200 ms/div)

Fig. 12. Measured output voltage V_o and current I_o waveforms under step-load changes from 20% to 100% of full load.

References

[1] H. D. Torresan, D. G. Holmes, and I. Shraga, “Auxiliary power supplies for high voltage converter systems,” *IEEE 35th Annual Power Electronics Specialists Conference*, 2004, pp. 645 – 651.

[2] H. D. Torresan, and D. G. Holmes, “A High Voltage Converter for Auxiliary Supply Applications using a Reduced Flying Capacitor Topology,” *IEEE 36th Power Electronics Specialists Conference*, 2005, pp. 1220 – 1226.

[3] Y. Jang, D.-L Dillman and M.-M Jovanovic, “ A new soft-switched PFC boost rectifier with integrated flyback converter for stand-by power,” *Transactions on Power Electronics*, Volume 21, Issue 1, pp.66-72, 2006.

[4] T. Higashi, T. Ninomiya and K. Harada, "On the Cross-Regulation of Multi-output Resonant Converters," *Proceedings of IEEE Power Electronics Specialists Conference*, 1988, pp. 18-25.

[5] Z. Hossain, Olejniczak, K.-C Burgers and J.-C balda, “Design of RCD Snubbers based upon Approximations to the Switching Characteristics: Part I. Theoretical Development,” *IEEE international Electric Machines and Drives Conference Record*, 1997, pp. TA2/6.1-TA2/6.3.

[6] W. McMurray, “Selection of Snubbers and Clamps to Optimize the Design of Transistor Switching Converters,” *IEEE Transactions on Industry Applications*, vol. 16, pp. 513 – 523, 1980.

[7] T. Ninomiya, T. Tanaka, and K. Harada, “Analysis and optimization of a nondissipative

LC turn-off snubber," *IEEE Transactions on Power Electronics*, vol. 3, pp. 147-156, April 1988.

[8] M. Milanovic, J. Korelic, A. Hren, F. Mihalic and P. Slibar, "The RC-RCD clamp circuit for fly-back converter," *Proceedings of the IEEE International Symposium on Industrial Electronics*, vol. 2, pp. 547-552, 2005.

[9] A. Hren, J. Korelic and M. Milanovic, "RC-RCD clamp circuit for ringing losses reduction in a flyback converter," *IEEE Transactions on Circuits and Systems II: Express Briefs*, vol. 53, no. 5, pp. 369-373, 2006.

[10] Z. Hossain, Olejniczak, K.-C Burgers and J.-C balda, "Design of RCD Snubber based upon Approximations to the Switching Characteristics: Part I. Theoretical Development," *Proceedings of IEEE International Electric Machines and Drives Conference*, pp. TA2/6.1-TA2/6.3, 1997.

[11] S.J. Finney, B.W. Williams and T.C. Green, "RCD snubber revisited," *IEEE Transactions on Industry Applications*, vol. 32, no. 1, pp. 155-160, 1996.

[12] M. Jinno, P.-Y. Chen and K.-C. Lin, "An Efficient Active LC Snubber for Multi-output Converters with Flyback Synchronous Rectifier," *Proceedings of the IEEE Power Electronics Specialist Conference*, vol. 2, pp. 622-627, 2003.

[13] T.-F. Wu and Y.-S. Lai, J.-C. Hung and Y.-M, Chen, "An Improved Boost Converter with Coupled inductors and Buck-Boost Type of Active Clamp," *Proceedings of Industry Applications Conference*, 2005, pp.639-644.

[14] S.-Y. Tseng, C.-.T Hsieh, H.-C. Lin, "Active Clamp Interleaved Flyback Converter with Single-Capacitor Turn-off Snubber for Stunning Poultry Applications," *Proceedings of IEEE Power Electronics and Drive System Conference*, 2007, pp. 1401-1408.